

Adsorption Equilibria of Nitrogen, Methane, and Ethane on BDH-Activated Carbon

Shaheen A. Al-Muhtaseb,* Fahmi A. Abu Al-Rub,[†] and Mohamed Al Zarooni

Department of Chemical and Petroleum Engineering, College of Engineering, United Arab Emirates (UAE) University, P.O. Box 17555, Al-Ain, United Arab Emirates

The adsorption equilibria of methane, ethane, and nitrogen on BDH-activated carbon was measured using a volumetric adsorption apparatus in the temperature range of (30 to 60) °C for nitrogen and methane and (40 to 60) °C for ethane. The absolute pressures covered in the measurements were in the range of (0 to 5) atm for methane and ethane and (0 to 8) atm for nitrogen. Overall, the adsorption isotherms showed a standard Langmuir-type isotherm behavior and were fitted favorably to the Langmuir equation in a predictive form. The isosteric heats of adsorption for each component on BDH-activated carbon were estimated based on these fittings. The experimental data were also fitted collectively to the Dubinin–Radushkevich equation. The fitting was satisfactory, and the fitting parameters were consistent with the adsorption affinities and total pore volume obtained from the experimental data.

Introduction

Vapor phase adsorption processes have recently received remarkable attention for use in industrial-scale applications due to their low cost of operation, ease of operation, and the ability to obtain high-purity products when using the appropriate adsorbents for separating gas mixtures.¹ Therefore, the modeling and simulation of such separation processes utilizing adsorption principles have received considerable interest in the past decade. Nonetheless, these simulations are impossible without knowledge of the equilibrium data for the adsorption of the concerned components on the selected adsorbent material.

The measurement of single-component adsorption equilibria over a relatively wide range of experimental conditions has many different uses. It is extremely useful for characterizing different adsorbent surfaces and investigating the nature of their interactions with the adsorbate molecules.^{2–5} Measured adsorption equilibrium data are also useful for evaluating the ability of different models to correlate the data over a wide range of conditions. Reliable correlations are also essential for estimating derived thermodynamic properties for the adsorption systems such as the isosteric heats of adsorption, the heat capacity of the adsorbed phase, and the entropy change upon adsorption.^{1–10} These thermodynamic properties along with non-isothermal adsorption equilibrium data are useful for simulating cyclic adsorption processes, such as temperature and pressure swing adsorption processes because the process conditions vary widely during cycling.

However, single-component adsorption equilibria measured over wide ranges of pressure and temperature on some commercially available adsorbents (such as BDH activated carbon) are quite rare in the literature. Much of the data that are available are either obsolete because the adsorbent is not being manufactured^{11–13} or measured over a relatively narrow range of experimental conditions with only a few data points obtained.

For this reason, many of the models in the literature may not be reliable when extrapolated over a broad range of conditions, such as those encountered in cyclic adsorption processes.

There are two common methods for measuring adsorption equilibria: gravimetric and volumetric methods. The gravimetric method relies on measuring the change of the adsorbent sample's weight upon the adsorption of the gas sample. It must be noted that the gravimetric measurements of the adsorption of light gases must consider a buoyancy correction. The volumetric adsorption apparatus is characterized by ease of design, construction, and operation. The volumetric methods depend on estimating the amount adsorbed through the difference between the amount in the gas phase before and after adsorption, which in turn are estimated using an equation of state.

In this work, the adsorption equilibrium data for the adsorption of nitrogen, methane, and ethane on BDH-activated carbon were measured over an industrially relevant range of temperatures (30 to 60 °C) and a wide range of pressures (0 to 8 atm) using a volumetric adsorption apparatus. The measurements covered a temperature range of (30 to 60) °C for nitrogen and methane and (40 to 60) °C for ethane. The absolute pressures covered in the measurements were in the range of (0 to 5) atm for methane and ethane and (0 to 8) atm for nitrogen. To the knowledge of the authors, adsorption equilibrium data for these systems have not been published before. These measurements are very helpful for estimating the thermodynamic properties of such systems and predicting the adsorption equilibria of mixtures constituted from these components.

Experimental Section

Chemicals. High-purity methane (grade 3.5) was provided by Air Products. Ethane with a purity of 99 % was provided by the Linde Chemicals Company. Nitrogen was a high-purity grade and provided by the Sharjah Oxygen Company.

BDH-activated carbon was received from the BDH Company in England in a granular form with a particle size 0.85–1.70 mm (10–18 mesh). It was labeled by the manufacturing company as “activated for gas adsorption”. Further characteristics of BDH-activated carbon were measured and estimated

* Corresponding author. E-mail: s.almuhtaseb@uaeu.ac.ae. Tel. +971-3-713-3545. Fax: +971-3-762-4262.

[†] Present address: Dept. of Chemical Engineering, Jordan University of Science and Technology, Irbid, Jordan.

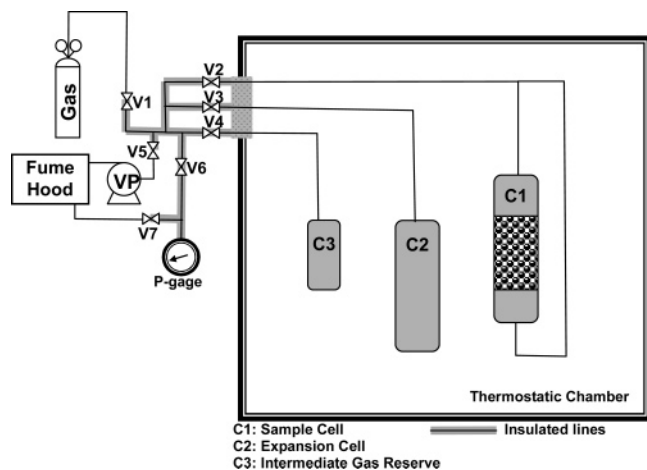


Figure 1. Schematic diagram of the volumetric adsorption apparatus.

using an ASAP-2010 apparatus and software. The BET surface area was $1220 \text{ m}^2 \cdot \text{g}^{-1}$ of which $1173 \text{ m}^2 \cdot \text{g}^{-1}$ was in the micropore region. The total pore volume was $534 \text{ cm}^3 \cdot \text{kg}^{-1}$ of which $479 \text{ cm}^3 \cdot \text{kg}^{-1}$ was in the micropore region. The BDH-activated carbon was used as received except for regeneration as explained in the following section.

Apparatus and Procedure. A volumetric adsorption apparatus was built at the UAE University. A schematic diagram of the apparatus used is shown in Figure 1. The adsorption and gas expansion cells are hosted in a thermostatic oven, which can be set in the temperature range of (30 to 220) °C with an accuracy of ± 1 °C. The apparatus was tested to be leak-proof for pressures up to 110 psig. The pressure gauge was an analogue type with a gauge pressure range of (−1 to 10) bar and an accuracy of 1 %. The vacuum pump (VP) had a vacuum rating of $20 \mu\text{m Hg}$ (20 mTorr). All cells and tubes were made of stainless steel, and the tubes outside the oven were insulated using glass wool. Cell C1 included 78.79 g of the dried BDH-activated carbon. The volume of cells C1 and C2 were 150 cm^3 , and that of C3 was 50 cm^3 . All the cells were obtained from Swagelok.

Prior to the first adsorption run, the dead volume in the cells was determined through expansion runs using nitrogen at 100 °C. Initially, nitrogen was charged with a known pressure to the expansion cells (C2 and C3), and then it was released to the adsorbent sample cell (C1). Adsorption was assumed to be negligible at that temperature. The total dead volume was calculated from the difference in pressure before and after expansion to the sample cell.

The activated carbon used was regenerated initially by placing it in an oven at 250 °C for 3 h. It was then placed in an evacuated desiccator (which also contains silica gel to adsorb humidity) until it reached room temperature. After that, the required sample was promptly weighed and placed in the adsorption cell. After placing the adsorption cell in its place in the apparatus, the adsorbent was regenerated by evacuating the whole apparatus to the gauge pressure of −1 bar, raising the temperature to 150 °C for 2 h, and monitoring the pressure to evacuate any desorbed gases. After that, the adsorbent was considered regenerated and ready for starting an adsorption experiment.

The adsorption runs were started from a regenerated adsorbent at a fixed temperature and a gauge pressure of −1 bar. Then, the gas cylinder valve V1 was opened to charge the expansion cells (C2, C3, or both) to an intermediate pressure step. Thermal equilibration was assumed to be reached in the expansion cell(s) 10 min after introducing the gas. After that, the gas was

allowed to expand to the sample cell where the adsorbent material was placed. The changes in pressure were monitored and recorded during this step. When the pressure in cell C1 became constant for about 30 min, adsorption equilibrium was reached and recorded for that pressure. The amount adsorbed at that point was calculated from the difference in the total moles in the gas phase present before and after the adsorption step. This constitutes one adsorption point. Further adsorption points were determined by closing the sample cell (C1), charging the expansion cell(s) with the gas to a higher intermediate pressure and repeating the same procedure that was used to obtain the first adsorption point. After reaching the maximum desired adsorption pressure, desorption experiments were obtained by closing the sample cell (C1), releasing some of the gas in the expansion cells to the fume hood, closing the expansion cells and then opening the sample cell to allow the gas to flow toward the lower pressure in the expansion cells. The pressure was monitored with time until it stabilized for about 30 min. That constituted one desorption point. This procedure was repeated with the use of the vacuum pump until the lowest desired pressure was reached.

After finishing the adsorption and desorption runs at the given temperature, the adsorbent was regenerated by evacuating the whole apparatus to the gauge pressure of −1 bar, raising the temperature to 150 °C for 2 h, and monitoring the pressure to evacuate any desorbed gases. After that, the adsorbent was considered regenerated and ready for another set of experiments at another temperature or with another gas.

Theory

The number of moles in the gas phase (n_g) can be calculated using an equation of state as

$$n_g = PV/ZRT \quad (1)$$

where P is the pressure, V is the gas volume, Z is the compressibility factor, R is the universal gas constant, and T is the absolute temperature. Z can be calculated from an equation of state such as the van der Waal's equation:

$$(-RT^3)Z^3 + (R^2BPT^2 + R^3T^3)Z^2 + (-RAPT)Z + (ABP^2) = 0 \quad (2)$$

where A and B are van der Waal's equation constants that are given by

$$A = \frac{27}{64} \frac{R^2 T_c^2}{P_c}; \quad B = \frac{RT_c}{P_c} \quad (3)$$

and T_c and P_c are respectively the critical temperature and pressure of the gas component.

Upon the adsorption of a gas species on an adsorbent, the differential amount adsorbed in one adsorption step according to the procedure detailed above can be calculated from the deviation of the number of moles in the gas phase:

$$\Delta n = \left(\sum_{j=1}^4 P_{f,j} V_{f,j} / Z_{f,j} - \sum_{j=1}^4 P_{i,j} V_{i,j} / Z_{i,j} \right) / RT \quad (4)$$

where the counter j stands for the three cells C1, C2, and C3 as well as the dead volume to correspond the j values of 1 through 4, respectively. The subscript "f" stands for the final state of the adsorption step (after reaching equilibrium) and the subscript "i" stands for the initial state of the adsorption step (before adsorption). The amount adsorbed at any pressure is estimated

from the summation of Δn for all the adsorption steps starting from the first adsorption step on the regenerated (cleaned up) adsorbent surface.

The adsorption equilibria (amount adsorbed n versus pressure at various temperatures) can be fitted using the Langmuir adsorption model, which depends on the concept of monolayer surface coverage and non-interacting adsorbed molecules:

$$\theta = \frac{n}{m} = \frac{bP}{1 + bP} \quad (5)$$

where θ is the fractional surface coverage, m is the monolayer saturation coverage limit (capacity) for the adsorbent surface, and b is an affinity factor which is given by

$$b = b_0 \exp(-\Delta H/RT) \quad (6)$$

where b_0 is a pre-exponential factor and ΔH is the average isosteric heat of adsorption.

At very low pressures, eq 5 approaches the Henry's law as

$$\theta^0 = \left(\lim_{P \rightarrow 0} \frac{\theta}{P} \right) P = bP \quad (7)$$

Since eq 7 is an equilibrium equation, with b standing for the equilibrium (Henry's law) coefficient, it should obey the van't Hoff equation, which can be expressed as

$$b = \exp\left(\frac{\Delta S^0}{R}\right) \exp\left(\frac{-\Delta H^0}{RT}\right) \quad (8)$$

where ΔS^0 and ΔH^0 are respectively the entropy and enthalpy change upon the adsorption on a clean surface. Knowing that the isosteric heat of adsorption corresponding to the Langmuir model is independent of loading or temperature, ΔH^0 can be approximated from ΔH . Consequently, ΔS^0 can be approximated by comparing eqs 8 and 6 as

$$\Delta S^0 = R \ln b_0 \quad (9)$$

The adsorption equilibrium data can also be fitted using a pore-filling model such as the Dubinin–Radushkevich (DR) equation¹⁴ as

$$W = W_0 \exp\left(-k \frac{\epsilon}{\beta}\right) \quad (10)$$

where W is the volume of adsorbed species, which is estimated as

$$W = nV_m \quad (11)$$

V_m is the molar volume of the adsorbed molecule (approximated from the liquid molar volume), W_0 is the estimated pore volume of the adsorbent, k is a fitting parameter, β is a coalescing factor that is intended as a shifting factor to bring the characteristic curves of all components on one adsorbent into a single curve, and ϵ is the adsorption potential that is equal to the work required to remove a molecule from its location in the adsorbed phase to the gas phase. The adsorption potential, ϵ , can be estimated for ideal gas molecules as

$$\epsilon = RT \ln\left(\frac{P^0}{P}\right) \quad (12)$$

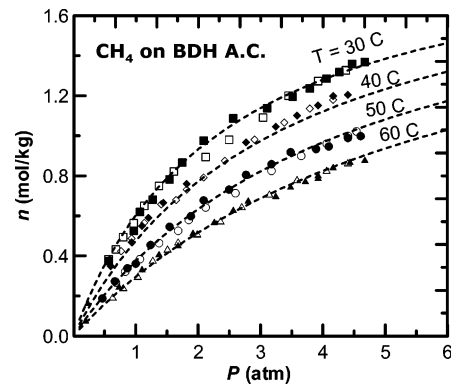


Figure 2. Equilibrium amount adsorbed (n) of methane on BDH-activated carbon as a function of temperature (T) and the system pressure (P). Lines indicate the fittings with the Langmuir model, and the filled and empty symbols indicate, respectively, adsorption and desorption data points.

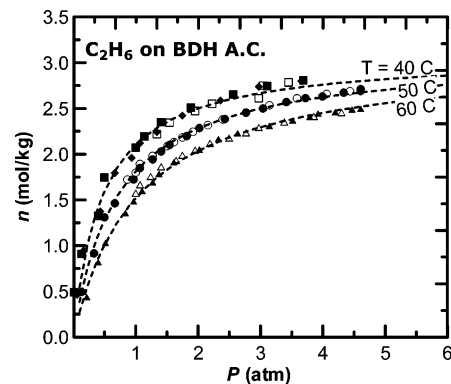


Figure 3. Equilibrium amount adsorbed (n) of ethane on BDH activated carbon as a function of temperature (T) and the system pressure (P). Lines indicate the fittings with the Langmuir model, and the filled and empty symbols indicate, respectively, adsorption and desorption data points.

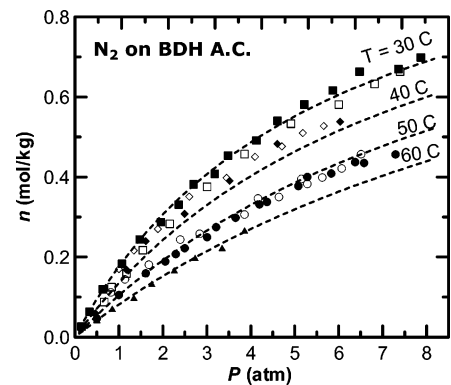


Figure 4. Equilibrium amount adsorbed (n) of nitrogen on BDH activated carbon as a function of temperature (T) and the system pressure (P). Lines indicate the fittings with the Langmuir model and the filled and empty symbols indicate, respectively, adsorption and desorption data points.

where P^0 is the vapor pressure of the adsorbed molecule at the corresponding temperature.

Results and Discussions

Figures 2 through 4 show the measured adsorption and desorption equilibrium data for methane, ethane, and nitrogen, respectively. It is clear from these figures that the isothermal adsorption and desorption data for each component are practically identical to each other and that these systems do not exhibit any hysteresis effect upon desorption. The measured adsorption and desorption equilibrium data of methane, ethane, and nitrogen

Table 1. Amount Adsorbed (n) of Methane on BDH-Activated Carbon versus Pressure (P) for the Temperature Range from $T = (30 \text{ to } 60) \text{ }^\circ\text{C}$.

P	n	P	n	P	n	P	n
atm	mol·kg ⁻¹	atm	mol·kg ⁻¹	atm	mol·kg ⁻¹	atm	mol·kg ⁻¹
$T = 30 \text{ }^\circ\text{C}$							
0.566	0.375	1.136	0.651	2.122	0.894	3.789	1.237
0.566	0.384	1.272	0.682	2.497	0.980	3.925	1.273
0.683	0.433	1.374	0.750	2.565	1.087	4.061	1.286
0.800	0.494	1.544	0.782	3.041	1.091	4.265	1.318
0.967	0.526	1.612	0.822	3.109	1.138	4.367	1.327
0.967	0.563	1.748	0.867	3.449	1.200	4.469	1.359
1.068	0.620	2.088	0.976	3.517	1.196	4.673	1.369
$T = 40 \text{ }^\circ\text{C}$							
0.599	0.349	1.204	0.590	2.088	0.792	3.585	1.101
0.766	0.424	1.408	0.658	2.429	0.875	3.789	1.136
0.933	0.468	1.442	0.665	2.769	0.967	3.925	1.152
0.933	0.488	1.646	0.679	2.905	0.981	4.163	1.198
1.102	0.550	1.816	0.760	3.245	1.046	4.163	1.180
1.136	0.566	1.816	0.731	3.381	1.066	4.401	1.205
$T = 50 \text{ }^\circ\text{C}$							
0.465	0.188	1.374	0.464	2.497	0.732	3.891	0.934
0.666	0.274	1.544	0.546	2.599	0.714	4.061	0.961
0.683	0.267	1.680	0.526	2.769	0.805	4.095	0.947
0.833	0.322	1.850	0.580	3.177	0.859	4.401	0.989
0.866	0.339	1.884	0.598	3.177	0.825	4.401	1.000
1.000	0.361	2.088	0.678	3.483	0.918	4.537	1.022
1.068	0.384	2.122	0.642	3.653	0.900	4.605	0.998
1.238	0.455						
$T = 60 \text{ }^\circ\text{C}$							
0.198	0.074	1.374	0.405	2.565	0.625	3.925	0.786
0.232	0.161	1.510	0.435	2.701	0.647	3.925	0.799
0.632	0.196	1.680	0.449	2.803	0.673	4.061	0.828
0.733	0.243	1.680	0.471	3.143	0.710	4.163	0.840
0.800	0.242	1.918	0.512	3.245	0.695	4.401	0.866
1.034	0.299	1.986	0.511	3.483	0.743	4.435	0.866
1.102	0.330	2.259	0.566	3.585	0.782	4.673	0.876
1.272	0.379	2.361	0.576	3.721	0.770		

Table 2. Amount Adsorbed (n) of Ethane on BDH-Activated Carbon versus Pressure (P) for the Temperature Range from $T = (40 \text{ to } 60) \text{ }^\circ\text{C}$

P	n	P	n	P	n	P	n
atm	mol·kg ⁻¹	atm	mol·kg ⁻¹	atm	mol·kg ⁻¹	atm	mol·kg ⁻¹
$T = 40 \text{ }^\circ\text{C}$							
0.031	0.478	0.432	1.374	1.068	2.122	2.361	2.587
0.064	0.464	0.666	1.794	1.340	2.243	2.973	2.738
0.165	0.946	0.933	1.959	1.748	2.422	3.653	2.800
0.165	0.939						
$T = 50 \text{ }^\circ\text{C}$							
0.131	0.494	1.272	1.943	2.020	2.286	3.585	2.610
0.332	0.916	1.272	1.982	2.156	2.318	3.721	2.613
0.499	1.310	1.408	2.029	2.395	2.381	3.993	2.631
0.666	1.463	1.510	2.089	2.429	2.384	4.061	2.659
0.866	1.722	1.544	2.102	2.769	2.453	4.333	2.672
0.967	1.723	1.612	2.132	2.769	2.456	4.435	2.688
1.000	1.798	1.748	2.183	3.041	2.500	4.605	2.690
1.068	1.848	1.816	2.198	3.143	2.534	4.605	2.712
1.068	1.892	1.918	2.245	3.415	2.570		
$T = 60 \text{ }^\circ\text{C}$							
0.215	0.427	1.272	1.683	2.190	2.119	3.517	2.358
0.399	0.809	1.374	1.774	2.327	2.155	3.789	2.397
0.516	1.019	1.408	1.863	2.497	2.177	3.857	2.413
0.833	1.346	1.612	1.904	2.633	2.218	3.925	2.433
0.967	1.474	1.646	1.933	2.769	2.235	4.197	2.451
1.000	1.575	1.748	1.988	2.973	2.293	4.299	2.456
1.068	1.667	1.952	2.045	3.143	2.301	4.469	2.479
1.102	1.589	2.020	2.040	3.381	2.352	4.605	2.487
1.238	1.757						

on BDH-activated carbon are shown in Tables 1 through 3, respectively.

Table 4 shows the fitting results of the Langmuir equilibrium model according to eqs 5, 6, and 9. The Langmuir equation

Table 3. Amount Adsorbed (n) of Nitrogen on BDH-Activated Carbon versus Pressure (P) for the Temperature Range from $T = (30 \text{ to } 60) \text{ }^\circ\text{C}$

P	n	P	n	P	n	P	n
atm	mol·kg ⁻¹	atm	mol·kg ⁻¹	atm	mol·kg ⁻¹	atm	mol·kg ⁻¹
$T = 30 \text{ }^\circ\text{C}$							
0.148	0.027	1.476	0.244	3.177	0.408	5.864	0.616
0.332	0.063	1.544	0.217	3.483	0.454	6.000	0.581
0.632	0.120	1.952	0.287	3.857	0.457	6.476	0.663
0.666	0.088	2.156	0.283	4.129	0.492	6.816	0.633
0.833	0.125	2.361	0.331	4.605	0.540	7.361	0.670
1.068	0.183	2.701	0.382	4.912	0.533	7.395	0.663
1.170	0.159	3.007	0.376	5.218	0.581	7.871	0.699
$T = 40 \text{ }^\circ\text{C}$							
0.465	0.059	1.612	0.240	3.449	0.398	4.707	0.477
1.000	0.170	1.884	0.270	3.517	0.391	5.184	0.510
1.170	0.168	2.497	0.308	4.095	0.451	5.660	0.528
1.340	0.216	2.599	0.351	4.605	0.483	6.034	0.538
$T = 50 \text{ }^\circ\text{C}$							
0.499	0.047	2.395	0.244	4.197	0.332	5.626	0.399
0.816	0.112	2.497	0.222	4.367	0.338	5.830	0.409
1.000	0.105	2.837	0.258	4.639	0.350	6.068	0.421
1.136	0.144	3.007	0.250	5.082	0.377	6.374	0.437
1.612	0.159	3.211	0.275	5.150	0.395	6.510	0.457
1.680	0.181	3.653	0.298	5.286	0.400	6.578	0.435
2.054	0.189	3.857	0.306	5.286	0.383	7.293	0.457
2.293	0.207	4.163	0.347				
$T = 60 \text{ }^\circ\text{C}$							
0.499	0.040	1.340	0.096	2.259	0.165	3.347	0.221
0.850	0.068	1.748	0.131	2.735	0.196	3.857	0.264

given in eqs 5 and 6 has only three fitting parameters for each component over the entire range of temperature. Therefore, it can be used to predict adsorption isotherms at temperatures other than those measured experimentally.

It can be noted from the values of the monolayer saturation limit m in Table 4 that BDH-activated carbon has a higher capacity for ethane as compared to methane, which in turn is characterized with a higher capacity than that of nitrogen. It should be noted, however, that these fits are applicable only within the ranges of pressure studied. The same trend can also be noted from the heats of adsorption where the adsorption of ethane is the most exothermic, followed by that of methane and then nitrogen. This means that ethane will experience the maximum reduction in its free energy upon adsorption on activated carbon.

Theoretically, the Langmuir constant b represents the equilibrium constant of an idealized adsorption process expressed as



where A is the adsorbate molecule in vapor phase, C* is the available adsorptive site of the BDH, and C*A is the site occupied by adsorbate. The sum of the numbers of C* and C*A is the total number of adsorbing sites, which is equivalent to the value of m . A larger value of the equilibrium constant b indicates a stronger adsorption on the adsorptive site. The results shown in Table 1 indicate that ethane has the largest value of the components studied, suggesting stronger interactions between ethane and the surface of BDH-activated carbon. A similar conclusion can be drawn by thermodynamic analysis using the entropy differences, which are presented between squared brackets in Table 4. The entropy differences ΔS^0 are all negative (spontaneous) and are of comparable magnitude. Nonetheless, the absolute value of the entropy difference for ethane is the biggest as compared to that of methane and nitrogen. This indicates strong interactions between the molecules of ethane

Table 4. Fitting Parameters of the Langmuir Adsorption Model and the Corresponding Average Relative Error (ARE^a) in the Amount Adsorbed

	nitrogen	methane	ethane
m (mol·kg ⁻¹) =	1.18	2.05	3.08
$10^6 \times b_0$ (atm ⁻¹) =	12.25 [-0.094] ^b	17.71 [-0.091] ^b	3.97 [-0.103] ^b
heat of adsorption (- ΔH /(kJ·mol ⁻¹)) =	24.12	25.38	34.37
ARE/% =	6.51	3.42	3.06

$$^a \text{ARE} = \frac{100}{N} \sum_{i=1}^N \left(\frac{|n_{\text{calc}} - n_{\text{exp}}|}{n_{\text{exp}}} \right)_i \text{ where } N \text{ is the total number of points for each component.}$$

^b Values between the square brackets denote the entropy variations upon adsorption on a clean adsorbent surface (ΔS^0) in kJ·mol⁻¹·K⁻¹ estimated by eq 9.

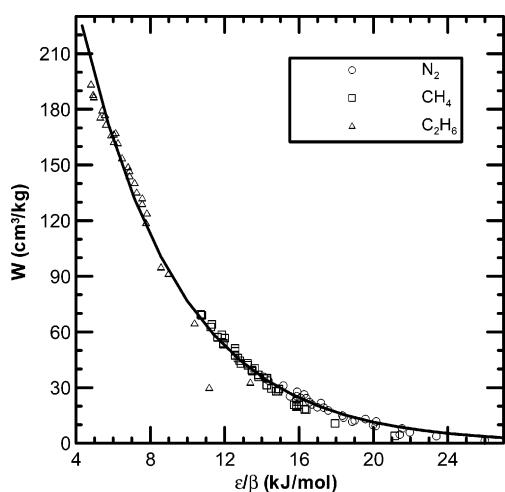


Figure 5. Characteristic curve fitting (line) for the non-isothermal adsorption equilibrium data of nitrogen (circles), methane (squares), and ethane (triangles) according to the DR equation. The number of symbols shown in this graph is reduced to improve its clarity.

Table 5. Fitting Parameters of the DR Equation and the Corresponding AREs^a for the Overall Set of Measured Data

W_0 (cm ³ ·kg ⁻¹) =	512.0
k =	0.190
β_{N_2} =	0.829
β_{CH_4} =	1.000
$\beta_{\text{C}_2\text{H}_6}$ =	1.447
ARE/% =	11.59

^a ARE is defined as in Table 4.

and the surface of the activated carbon. On the other hand, methane and nitrogen both exhibit comparable values of their entropy differences. Therefore, they do not have much difference in their interaction with the adsorbent, which minimizes the competition between them.

Figure 5 shows that the measured non-isotherm adsorption equilibrium data of nitrogen, methane, and ethane can be collectively fitted satisfactorily to the DR equation. The saturation pressures and V_m values were calculated as functions of temperature using parameters presented by Henley and Seader.¹⁵ The critical properties were obtained from *Perry's Chemical Engineering Handbook*.¹⁶ The corresponding fitting parameters and the average relative error (ARE) are listed in Table 5. The β value for methane was fixed at 1.000 as a reference, and those of nitrogen and ethane were optimized along with the other fitting parameters to result in the minimum sum of squared deviations between the experimental and calculated values. The obtained results were in fundamental agreement with published observations on the relationship between β and the adsorption affinity.¹⁷ It is noteworthy that this relationship is shown in this work to be directly proportional to the affinity, while in a previous work¹⁵ it was inversely proportional. This difference

Table 6. Comparison between the Langmuir Adsorption Isotherm's Affinity Parameter (b) for Various Activated Carbon Adsorbents at (40, 60, and 80) °C

adsorbent	$T = 40$ °C	$T = 60$ °C	$T = 80$ °C
BPL	0.046	0.032	0.022
Nuxite-AL	0.067	0.055	0.046
Columbia-G	0.099	0.054	0.032
BAX-1100	0.121	0.081	0.056
PCB	0.125	0.078	0.052
Columbia-L	0.198	0.130	0.090
Atriton resistant beads	0.207	0.137	0.096
BDH	0.303	0.169	0.101
Fiber Carbon KF-1500	0.381	0.247	0.169

is believed to be a result of using the molar volume in the previous work as a complementary counterpart to the coalescing factor. Table 5 shows that the adsorption affinity (or β value) of the adsorption on BDH-activated carbon is highest for ethane, followed by methane, and then nitrogen. This observation is consistent with that obtained previously from the Langmuir adsorption isotherm model. The total pore volume of the BDH activated carbon was estimated from the W_0 value of the DR equation as 512 cm³·kg⁻¹. This value compares favorably to the measured value (534 cm³·kg⁻¹) with a percentage relative error of 4.1 %. This adds credence to the measured adsorption equilibrium data.

An evaluation of BDH-activated carbon's affinity for the adsorption of hydrocarbon vapors is presented in Table 6, which shows the Langmuir adsorption isotherm's affinity parameter (b) for methane on various activated carbon adsorbents at (40, 60, and 80) °C. The comparison is done versus BAX-1100,¹⁷ BPL,¹⁸ PCB,¹⁸ Nuxite-AL,¹⁸ Columbia-L,¹⁸ Columbia-G,¹⁸ Atriton Resistant Beads,¹⁸ and Fiber Carbon KF-1500¹⁸ activated carbons. The b values corresponding to the BDH-activated carbon were always second to those corresponding to Fiber Carbon KF-1500 activated carbon. The high b values indicate that BDH-activated carbon has a remarkable affinity for adsorbing volatile organic compounds.

Conclusions

The adsorption equilibria of methane, ethane, and nitrogen on BDH-activated carbon has been measured using a volumetric adsorption apparatus in the temperature range of (30 to 60) °C for nitrogen and methane and (40 to 60) °C for ethane. The absolute pressures covered in the measurements were in the range of (0 to 5) atm for methane and ethane and (0 to 8) atm for nitrogen. At any specific condition, BDH-activated carbon showed the highest affinity and capacity for adsorbing ethane, followed by methane, and then nitrogen.

The measured adsorbed equilibria were fitted satisfactorily to a temperature-dependent form of the Langmuir isotherm model. The fitting resulted in a reasonable estimation of the isosteric heat of adsorption, and it can be used practically for

predicting the adsorption equilibria of multicomponent mixtures composed of combinations of methane, ethane, and nitrogen on BDH-activated carbon.

The DR potential theory model was also used to obtain a unified characteristic curve for the adsorbed components on the BDH-activated carbon. The fitting parameters for the DR equation led to consistent affinities and total pore volume as those estimated from the experimental data.

Acknowledgment

The authors acknowledge the help of the technicians Hasan Kamal Ahmad, Ibrahim Al-Maghrabi, and Dr. Ali Dowaidar for building the adsorption setup and conducting the adsorption experiments. A student, Mohammed Y. Haik, also helped in conducting the adsorption experiments.

Literature Cited

- (1) Ruthven, D. M. *Principles of Adsorption and Adsorption Processes*; Wiley: New York, 1984.
- (2) Jaroniec, M.; Madey, R. *Physical Adsorption on Heterogeneous Solids*; Elsevier: New York, 1988.
- (3) Rudzinski, W.; Everett, D. H. *Adsorption of Gases on Heterogeneous Surfaces*; Academic Press: London, 1992.
- (4) Masel, R. I. *Principles of Adsorption and Reaction on Solid Surfaces*; John Wiley and Sons: New York, 1996.
- (5) Olivier, J. P. Characterization of energetically heterogeneous surfaces from experimental adsorption isotherms. In *Surfaces of Nanoparticles and Porous Materials*; Schwarz, J. A., Contescu, C. I., Eds.; Marcel Dekker: New York, 1999.
- (6) Sircar, S. Isothermic heats of multicomponent gas adsorption on heterogeneous adsorbents. *Langmuir* **1991**, *7*, 3065.
- (7) Ritter, J. A.; Al-Muhtaseb, S. A. New model that describes adsorption of laterally interacting gas mixtures on random heterogeneous surfaces. 1. Parametric study and correlation with binary data. *Langmuir* **1998**, *14*, 6528.
- (8) Sircar, S.; Rao, M. B. Heat of adsorption of pure gas and multicomponent gas mixtures on microporous adsorbents. In *Surfaces of Nanoparticles and Porous Materials*; Schwarz, J. A., Contescu, C. I., Eds.; Marcel Dekker: New York, 1999; pp 501–528.
- (9) Al-Muhtaseb, S. A.; Ritter, J. A. Roles of surface heterogeneity and lateral interactions on the isosteric heat of adsorption and adsorbed phase heat capacity. *J. Phys. Chem. B* **1999**, *103*, 2467–2479.
- (10) Al-Muhtaseb, S. A.; Holland, C. E.; Ritter, J. A. Adsorption of C₁ to C₇ normal alkanes on BAX activated carbon. 2. Statistically optimized approach for deriving thermodynamic properties from the adsorption isotherm. *Ind. Eng. Chem. Res.* **2001**, *40* (1), 319–337.
- (11) Szepešy, L.; Illes, V. Adsorption of gases and gas mixtures. I. Measurement of the adsorption isotherms of gases on active carbon up to pressures of 1000 Torr. *Acta Chim. Hung. Tomus* **1963**, *35*, 37.
- (12) Szepešy, L.; Illes, V. Adsorption of gases and gas mixtures. II. Measurement of the adsorption isotherms of gases on active carbon under pressures of 1 to 7 atm. *Acta Chim. Hung. Tomus* **1963**, *35*, 53.
- (13) Szepešy, L.; Illes, V. Adsorption of gases and gas mixtures. III. Investigation of the adsorption equilibria of binary gas mixtures. *Acta Chim. Hung. Tomus* **1963**, *35*, 245.
- (14) Yang, R. T. *Gas Separation by Adsorption Processes*; Imperial College Press: Singapore, 1997.
- (15) Henley, E. J.; Seader, J. D. *Equilibrium-Stage Separations in Chemical Engineering*; John-Wiley and Sons: New York, 1981.
- (16) Perry, R. H.; Green, D. W. *Perry's Chemical Engineers' Handbook*; Mc-Graw Hill: New York, 1999.
- (17) Holland, C. E.; Al-Muhtaseb, S. A.; Ritter, J. A. Adsorption of C₁ to C₇ normal alkanes on BAX activated carbon. 1. Potential theory correlation and adsorbent characterization. *Ind. Eng. Chem. Res.* **2001**, *40* (1), 338–346.
- (18) Valenzuela, D. P.; Myers, A. M. *Adsorption Equilibrium Data Handbook*; Prentice Hall: Englewood Cliffs, NJ, 1989.

Received for review May 15, 2006. Accepted October 21, 2006. The authors gratefully acknowledge financial support from the UAE University under the individual research grant number 04-02-7-11/05.

JE060215+